Supporting Information

Enhancement of Triplet-Sensitized Upconversion in Rigid Polymers via Singlet Exciton Sink Approach

Steponas Raišys,[a] Saulius Juršėnas,[a] Yoan C. Simon,[bc] Christoph Weder [b] and Karolis Kazlauskas*[a]

a *Institute of Photonics and Nanotechnology, Vilnius University, Saulėtekio av. 3, LT-10257 Vilnius, Lithuania.*

b *Adolphe Merkle Institute, University of Fribourg, Chemin des Verdiers 4, CH-1700 Fribourg, Switzerland*

c *School of Polymer Science and Engineering, University of Southern Mississippi, 118 College Drive #5050, Hattiesburg, Mississippi 39406, United States*

Corresponding Author

*E-mail: karolis.kazlauskas@ff.vu.lt

Experimental section

Materials: Chemicals including DPA, PtOEP, PMMA and PCBM were purchased from Sigma-Aldrich and were used as received. The singlet exciton sink PE was synthesized according to the previously published procedures.[1]

***Preparation of the Upconverting Films*:** Upconverting films were prepared following a previously reported melt-processing procedure.[2] First, PMMA matrix (30 mg), DPA emitter (15 – 40 wt%), and PtOEP sensitizer (5×10^{-3} – 1 wt%) were dissolved at the desired ratio in chlorobenzene (300 µL) by stirring for 4 h at 65°C. Here wt% of a substance is defined as a weight percentage relative to the total weight content of the mixture. For evaluation of singlet exciton diffusion in DPA/PtOEP/PMMA films, varying amounts of PCBM quencher (0 – 2 wt%) were additionally introduced. To demonstrate the singlet exciton sink approach, a pyreneethylene derivative (PE) was also added at concentrations ranging from 10^{-3} to 1 wt%. The mixtures were drop-casted on pre-cleaned 150-µm-thick glass substrate at 200°C and left for 30 min to evaporate the solvent. Then, the films were covered with another glass slide and hot-pressed in a Carver press at 240°C under a pressure of ~100 kg/cm^2 for 5 min. The samples were then removed from the press and immediately cooled in an ice-bath. The immediate cooling was performed to induce a rapid thermal quenching below T_g, and allow for kinetic trapping of homogeneous mixtures, thus suppressing substantial emitter aggregation even at high dye content.[3]

DPA concentration in the UC films was set to 15, 20, 25, 30, 35 and 40 wt%, whereas the concentration of PtOEP was varied in a more continuous manner from 5×10^{-3} to 1 wt%. Additional sets of reference films containing only the emitter (DPA/PMMA) and only the sensitizer (PtOEP/PMMA) were also prepared using the same melt-processing technique.

Photophysical Measurements: Absorption spectra of the films were recorded using a UV−vis−near-IR spectrophotometer Lambda 950 (PerkinElmer). The emission of the samples was caused by

excitation at 405 and 532 nm, using semiconductor laser diodes and measured using a back-thinned CCD spectrometer PMA-11 (Hamamatsu). The fluorescence quantum yield was estimated by utilizing an integrating sphere (Sphere Optics) coupled to the CCD spectrometer via an optical fiber. Fluorescence transients of the samples were measured by using a time-correlated single photon counting system PicoHarp 300 (Picoquant), which utilized a pulsed semiconductor laser diode (repetition rate - 1 MHz, pulse duration - 70 ps, emission wavelength - 375 nm) as an excitation source. The phosphorescence spectrum of PE was recorded using a time-gated intensified CCD camera New iStar DH340T (Andor) coupled with a spectrograph SR-303i (Shamrock), whereas a wavelength-tunable optical parametric amplifier tuned to 415 nm and pumped by a pulsed Nd^{3+}:YAG laser (EKSPLA) (pulse duration – 5 ns, repetition rate – 1 kHz) served as an excitation source. Phosphorescence measurements of PE dispersed in PMMA at 0.15 wt% were performed at a temperature of 10 K using closed cycle helium cryostat 204N (Cryo Industries) with sample in exchange gas.
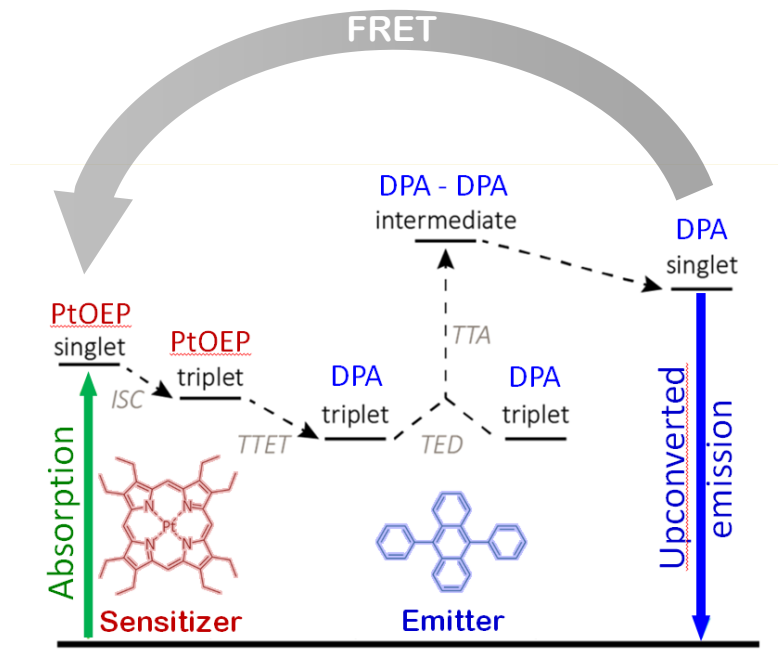
Figure S1. The pathway of TTA-UC process consists of the following events: i) low-energy photon absorption by a sensitizer, ii) intersystem crossing (ISC) to triplet manifold followed by triplet energy transfer (TTET) to emitter molecules, iii) triplet exciton diffusion (TED) and formation of encounter complex, iv) population of singlet excited state of an emitter by means of triplet-triplet annihilation (TTA) followed by higher-energy photon emission.

Gray arrow indicates long–range Förster resonant energy transfer (FRET) of upconverted emitter singlets back to the sensitizer.
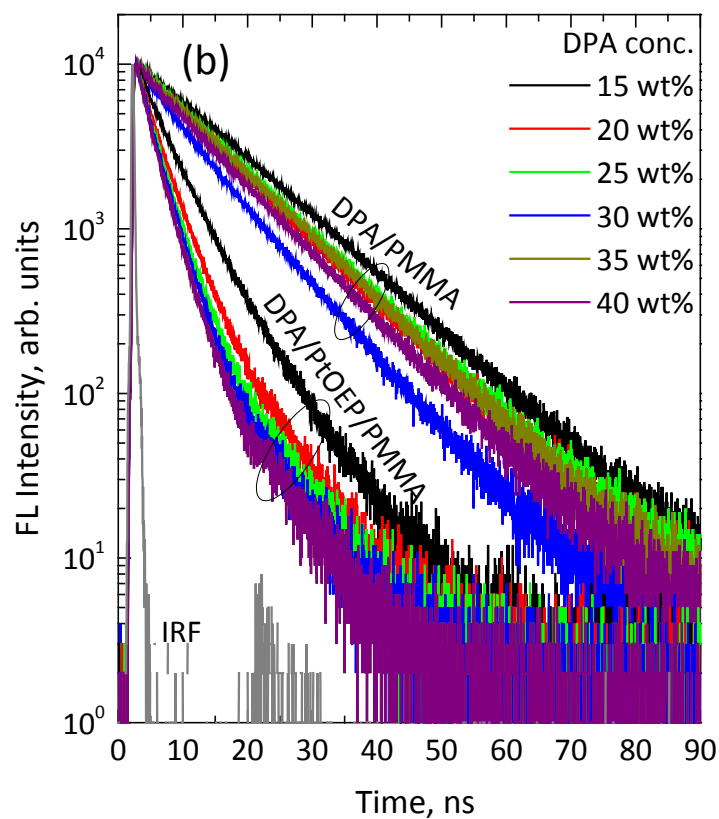
Figure S2. Fluorescence decay of DPA/PMMA and DPA/PtOEP/PMMA ($c_{PtOEP} = 0.05$ wt%) films at different DPA concentrations.
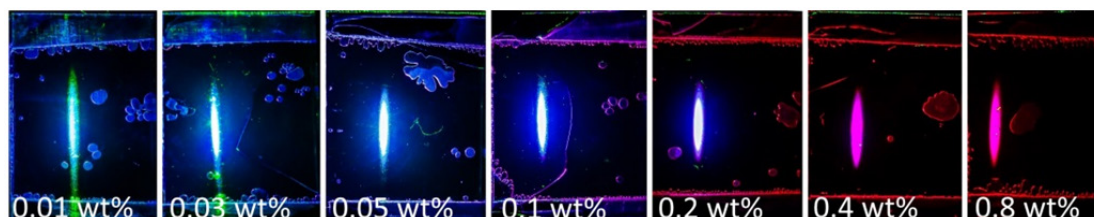

Figure S3. Photographs of the upconverting DPA/PtOEP/PMMA films containing 25 wt% of DPA and at different PtOEP concentrations (indicated). Excitation wavelength – 532 nm.
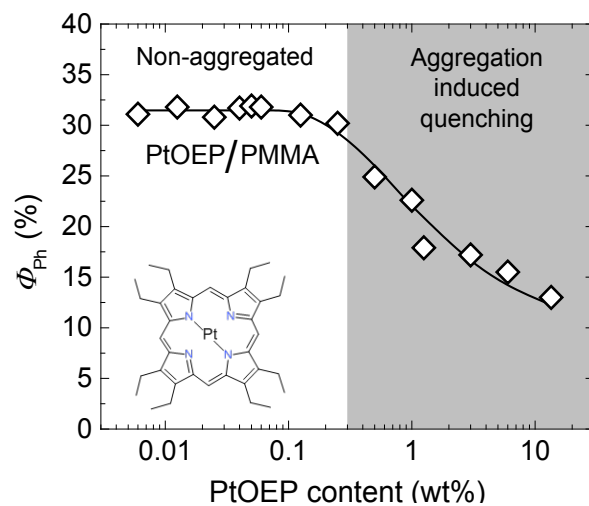
Figure S4. Phosphorescence quantum yield of melt-processed PtOEP/PMMA films as a function of PtOEP concentration. The line is a guide to the eye. Shaded region indicates aggregation induced quenching of PtOEP.
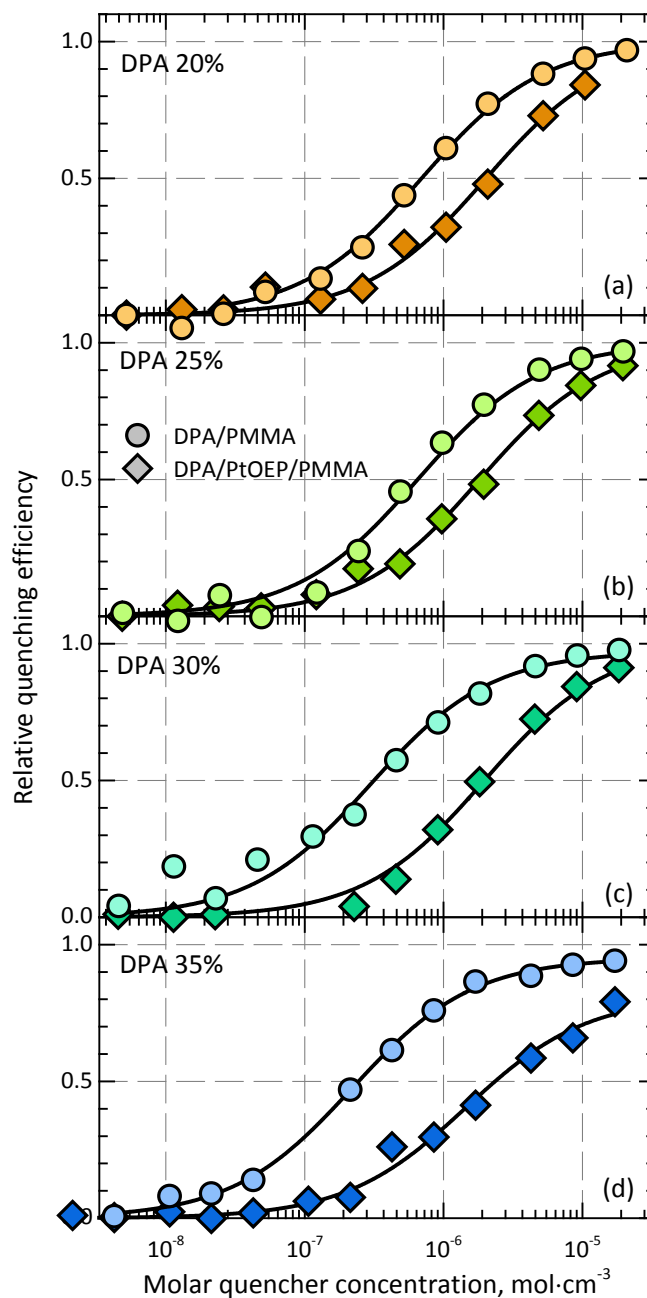
Figure S5. Relative quenching efficiency *vs* molar quencher concentration of DPA/PMMA and DPA/PtOEP/PMMA (c_{PtOEP} = 0.05 wt%) films at different DPA concentrations: (a) 20 wt%, (b) 25 wt%, (c) 30 wt%, (d) 35 wt%. Lines show Stern-Volmer fits. For the fluorescence quenching experiments the excitation wavelength was 405 nm.

Quenching efficiency curves were modelled using the Stern–Volmer formalism and "hindered access model",[4] which implies that only a fraction (f_a) of molecules is accessible to the quencher due to its aggregation at higher concentrations. According to the formalism relative quenching efficiency can be written as

$$\frac{I_0 - I_q}{I_0} = f_a - \frac{f_a}{1 + K_{SV}[Q_c]} \tag{1}$$

Here I_0 and I_q is the time-integrated emission intensity without and with a quencher, respectively, $[Q_c]$ is a quencher concentration and K_{SV} is Stern-Volmer constant, which can be expressed as

$$K_{SV} = k_q \tau, \tag{2}$$

where k_q is quenching rate coefficient and τ - exciton lifetime. The exciton quenching rate is proportional to the probability (P) that a quenching reaction will occur when exciton collides with the quencher ($P=0.5$ for FRET at R_0), to the reaction radius of the two colliding species (r), to diffusion coefficient (D) and Avogadro's number (N_A):

$$k_q = 4\pi r P D N_A. \tag{3}$$

In Eq. (3), r was calculated by taking into account Förster resonant energy transfer from DPA to PCBM, i.e.

$$r^6 = (R_0 + r_{PCBM})^6 = \frac{9\Phi_{FL}\kappa^2}{128\,\pi^5 n^4} \int \lambda^4 F_D(\lambda)\sigma_A(\lambda)d\lambda + r_{PCBM}$$
$$= \frac{9\Phi_{FL}\kappa^2}{128\,\pi^5 n^4} J(\lambda) + r_{PCBM}, \tag{4}$$

where r_{PCBM} is PCBM quencher radius (=0.5 nm), Φ_{FL} is the fluorescence quantum yield, κ is dipole orientation factor, n is the refraction index, λ is the wavelength, F_D is the normalized fluorescence spectrum, σ_A is absorption cross-section, and $J(\lambda)$ is spectral overlap integral. κ was assumed to be $0.845\sqrt{2/3}$ for amorphous film with randomly oriented dipoles.[5]

The singlet exciton diffusion length was obtained from:

$$L_D = \sqrt{ZD\tau}, \tag{5}$$

where Z equals 3 in the case of three-dimensional diffusion.[6]

Table S1. Stern-Volmer fitting parameters used for the quantitative evaluation of singlet exciton diffusion in the DPA/PtOEP/PMMA films

DPA wt%	PtOEP wt%	R_0 nm	K_{SV} $cm^3 \times mol^{-1}$	k_q $cm^3 mol^{-1} s^{-1}$	D $cm^2 \times s^{-1}$	$<\tau>$ ns	L_D nm	f_a
		w/o PtOEP						
20	0	5.72	$1.4\times10^6\ (\pm8.2\times10^4)$	1.6×10^{14}	6.7×10^{-5}	9.1	13.5	1.0
25	0	5.61	$1.5\times10^6\ (\pm1.8\times10^5)$	1.8×10^{14}	7.8×10^{-5}	8.6	14.1	1.0
30	0	5.61	$3.4\times10^6\ (\pm5.2\times10^5)$	3.5×10^{14}	1.5×10^{-4}	9.7	20.9	0.9
35	0	5.52	$4.5\times10^6\ (\pm2.4\times10^5)$	5.2×10^{14}	2.3×10^{-4}	8.8	24.5	0.9
		w/ PtOEP						
20	0.05	5.72	$4.9\times10^5\ (\pm6.9\times10^4)$	1.3×10^{14}	5.7×10^{-5}	3.7	7.9	1.0
25	0.05	5.61	$5.5\times10^5\ (\pm5.9\times10^4)$	1.7×10^{14}	7.2×10^{-5}	3.3	8.5	1.0
30	0.05	5.61	$5.1\times10^5\ (\pm5.7\times10^4)$	1.8×10^{14}	7.9×10^{-5}	2.8	8.1	0.9
35	0.05	5.52	$6.9\times10^5\ (\pm9.2\times10^4)$	2.5×10^{14}	1.1×10^{-4}	3.1	9.5	0.8

FRET rates and Forster radii for the DPA → PtOEP, DPA → PE, PE → DPA and PE → PtOEP processes at the fixed DPA and PtOEP concentrations of 25wt% and 0.01wt% (used throughout this work), respectively, were estimated from these relationships

$$k_F = \frac{1}{\tau}\left(\frac{R_0}{d}\right)^6,$$

$$R_0^6 = \frac{9\Phi_F \kappa^2}{128\,\pi^5 n^4}\int \lambda^4 F_D(\lambda)\sigma_A(\lambda)d\lambda = \frac{9\Phi_F \kappa^2}{128\,\pi^5 n^4}\,J(\lambda),$$

Table S2. Parameters used for calculating FRET rates and Forster radii for DPA → PtOEP, DPA → PE, PE → DPA and PE → PtOEP processes.

DPA conc. in PMMA wt%[*]	J nm^6	Φ_{FL} %	κ	n	R_0 nm	d nm	τ ns	k_F s^{-1}
DPA → PtOEP								
25	$1.52 \cdot 10^8$	76	0.69	1.6	7.60	1.23	11.5	$4.93 \cdot 10^{12}$
DPA → PE								
25	$3.41 \cdot 10^8$	76	0.69	1.6	8.69	1.23	11.5	$1.10 \cdot 10^{13}$
PE → PtOEP								
25[**]	$2.41 \cdot 10^8$	69	0.69	1.6	8.08			
PE concentration in 25wt% DPA, 0.01wt% PtOEP PMMA blend								
0.001					8.08	21.22	1.82	$1.67 \cdot 10^6$
0.002					8.08	20.81	1.82	$1.88 \cdot 10^6$
0.005					8.08	19.73	1.82	$2.58 \cdot 10^6$
0.01					8.08	18.35	1.82	$4.00 \cdot 10^6$
0.05					8.08	13.39	1.82	$2.65 \cdot 10^7$
0.2					8.08	9.00	1.82	$2.87 \cdot 10^8$
0.4					8.08	7.23	1.82	$1.07 \cdot 10^9$
0.8					8.08	5.77	1.82	$4.12 \cdot 10^9$
1.6					8.08	4.60	1.82	$1.62 \cdot 10^{10}$
PE → DPA								
25[**]	$1.70 \cdot 10^5$	69	0.69	1.6	2.41			
PE concentration in 25wt% DPA, 0.01wt% PtOEP PMMA blend								
0.001					2.41	1.23	1.82	$3.18 \cdot 10^{10}$
0.002					2.41	1.23	1.82	$3.18 \cdot 10^{10}$
0.005					2.41	1.23	1.82	$3.18 \cdot 10^{10}$
0.01					2.41	1.23	1.82	$3.18 \cdot 10^{10}$
0.05					2.41	1.23	1.82	$3.18 \cdot 10^{10}$
0.2					2.41	1.23	1.82	$3.18 \cdot 10^{10}$
0.4					2.41	1.23	1.82	$3.19 \cdot 10^{10}$
0.8					2.41	1.23	1.82	$3.19 \cdot 10^{10}$
1.6					2.41	1.22	1.82	$3.21 \cdot 10^{10}$

[*] - PtOEP concentration 0.01wt%.
[**] - PE concentration 0.01wt%.
J – spectral overpal integral
Φ_{FL} – fluorescence quantum yield
κ – dipole orientation factor
n – refractive index
τ – exciton lifetime
R_0 – Förster radius
k_F – Förster energy transfer rate

Förster energy transfer rates (s^{-1})

$$\text{PtOEP} \xleftarrow[10^6 - 10^{10}]{} \text{PE}$$

DPA

$\sim1\cdot10^{13}$

$\sim3\cdot10^{10}$

$h\nu$ $\sim1\cdot10^8$
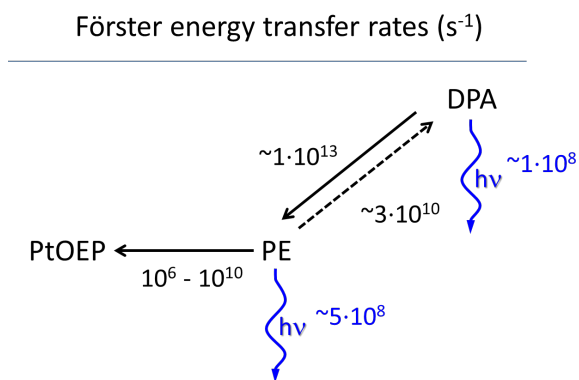
$h\nu$ $\sim5\cdot10^8$

Figure S6. Schematic drawing of the FRET rates for DPA/PtOEP/PE/PMMA films at the fixed DPA and PtOEP concentrations of 25wt% and 0.01wt%, respectively, and at different PE concentrations 0.001 − 1.6 wt%.
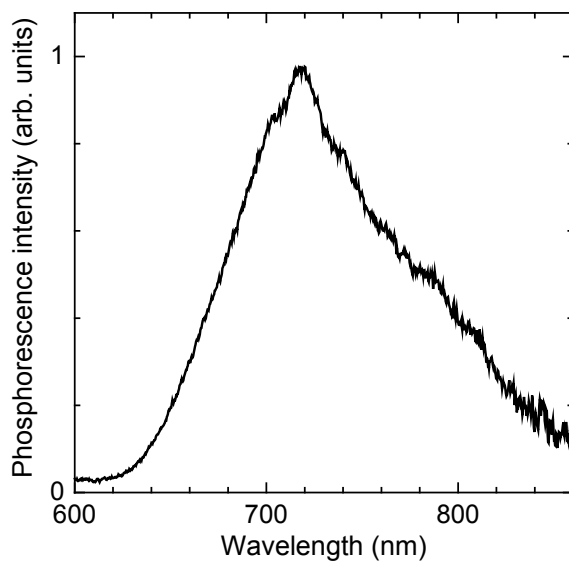

Figure S7. Phosphorescence spectrum of the singlet sink PE in PMMA (c_{sink} = 0.15 wt%) measured at 10K. Excitation wavelength - 415 nm.
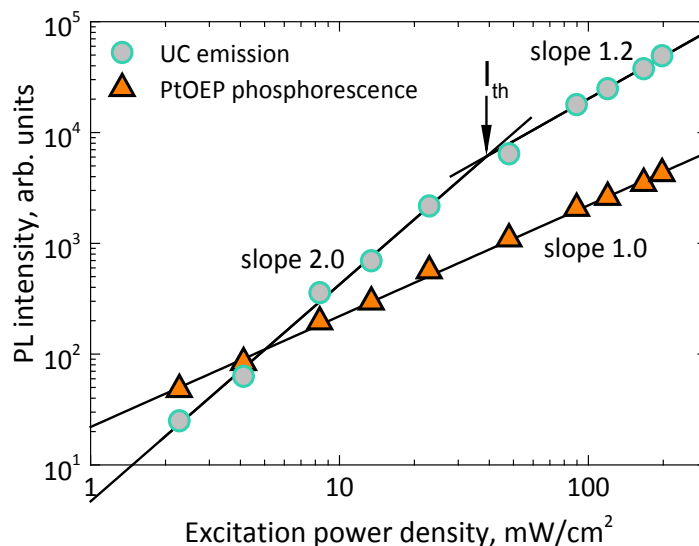
Figure S8. UC and PtOEP phosphorescence intensity as a function of excitation power density of the film DPA/PtOEP/sink/PMMA (c_{DPA} = 25 wt%, c_{PtOEP} = 0.01 wt%, c_{sink} = 0.01 wt%). Excitation wavelength - 532 nm. The arrow indicates the threshold density, where the UC intensity switches from quadratic to linear regime.

References

1 J. Gupta, S. Vadukumpully and S. Valiyaveettil, *Polymer*, 2010, **51**, 5078–5086.
2 S. H. Lee, J. R. Lott, Y. C. Simon and C. Weder, *J. Mater. Chem. C*, 2013, **1**, 5142–5148.
3 S. Raišys, K. Kazlauskas, S. Juršėnas and Y. C. Simon, *ACS Appl. Mater. Interfaces*, 2016, **8**, 15732–15740.
4 H.-Y. Hsu, J. H. Vella, J. D. Myers, J. Xue and K. S. Schanze, *J. Phys. Chem. C*, 2014, **118**, 24282–24289.
5 M. Z. Maksimov and I. M. Rozman, *Optics and Spectroscopy*, 1962, **12**, 337.
6 J. D. A. Lin, O. V. Mikhnenko, J. Chen, Z. Masri, A. Ruseckas, A. Mikhailovsky, R. P. Raab, J. Liu, P. W. M. Blom, M. A. Loi, C. J. García-Cervera, I. D. W. Samuel and T.-Q. Nguyen, *Mater. Horiz.*, 2014, **1**, 280–285.